Article

Not peer-reviewed version

Using Multiple Gcm Models to Reduce Uncertainties in Assessment of the Effect of Future Climate Change on Cotton Growth and Water Consumption in China

Ruixue Yuan , Keyu Wang , Dandan Ren , Zhaowang Chen , Baosheng Guo , Haina Zhang , Dan Li , Cunpeng Zhao , Shumin Han , Huilong Li , Shuling Zhang , De Li Liu , Yanmin Yang *

Posted Date: 31 March 2025

doi: 10.20944/preprints202503.2226.v1

Keywords: Climatic change; cotton; Apsim; model; ET

 doi:10.20944/preprints202503.2226.v1

Article

Using Multiple GCM Models to Reduce Uncertainties in Assessment of the Effect of Future Climate Change on Cotton Growth and Water Consumption in China

Yanmin Yang [1], Keyu Wang [2†], Dandan Ren [3†], Baosheng Guo [4], Haina Zhang [4], Dan Li [4], Cunpeng Zhao [4], Zhaowang Chen [1,5,*], Ruixue Yuan [1,5], Shumin Han [1], Huilong Li [1], Shuling Zhang [5] and De Li Liu [6]

[1] Center for Agricultural Resources Research, Institute of Genetics and Developmental Biology, Chinese Academy of Sciences, Shijiazhuang 050021, China
[2] Liaocheng Hydrology Center, Liaocheng 252000, China
[3] School of Resources and Environment, College of Carbon Neutrality, Linyi University, Linyi 276000, China
[4] Cotton Institute, Hebei Academy of Agriculture and Forestry Sciences, Shijiazhuang 050051, China
[5] College of Life Sciences, Hebei University, Baoding 071002, China
[6] NSW Department of Primary Industries, Wagga Wagga Agricultural Institute, PMB, Wagga Wagga, NSW 2650, Australia
* Correspondence: ymyang@sjziam.ac.cn
† These authors contributed equally to this work.

Abstract: Global Climate Models (GCMs) are a primary source of uncertainty in assessing climate change impacts on agricultural production, especially when relying on limited models. Considering China's vast territory and diverse climates, this study utilized 22 GCMs and selected three representative cotton-producing regions: Aral (northwest inland), Wangdu (Yellow River basin), and Changde (Yangtze River basin). Using the APSIM model, we simulated climate change effects on cotton yield, water consumption, uncertainties, and climatic factor contributions. Results showed significant variability driven by different GCMs, with uncertainty increasing over time and under radiation forcing. Spatial variations in uncertainty were observed: Wangdu exhibited highest uncertainties in yield and phenology, while Changde had the greatest uncertainties in ET and irrigation amount. Key factors affecting yield varied regionally—daily maximum temperature and precipitation dominated in Aral; precipitation was a major negative factor in Wangdu; and maximum temperature and solar radiation were critical in Changde. This study provides scientific support for developing climate change adaptation measures tailored to cotton production across different regions.

Keywords: Climatic change; cotton; Apsim; model; ET

1. Introduction

1.1. Climate Projection Models and Their Uncertainties

Global Climate Models (GCMs) are tools used to project future climate changes based on historical climate observation data, capable of simulating climate variations across different spheres of the Earth. These climate projection models carry inherent uncertainties, which manifest in several ways: (i) Model structure and parameterization: This includes limitations intrinsic to the model structure, parameterization schemes, assumptions, and calibration processes [1]; (ii) Idealized conditions: The models are built under idealized conditions and thus struggle to accurately simulate the impacts of human activities, geographical locations, and atmospheric environments. Different

 doi:10.20944/preprints202503.2226.v1

GCMs exhibit varying performances across distinct regions [2]. In site-specific climate change projections, GCMs are employed to drive process-based models for assessing the effects of climate change [3-5]. However, discrepancies arise due to the varying temporal and spatial resolutions among different GCMs, leading to errors. Consequently, a common approach to reduce these errors and uncertainties in a given study area is to utilize an ensemble of multiple GCMs [6, 7]. This ensemble method emphasizes the importance of integrating multiple models to enhance the reliability and accuracy of climate projections, thereby mitigating the uncertainties associated with individual models.

1.2. Application of Crop Models For Future Climate Impact Assessment

Crop models are extensively employed for assessing the impacts of future climate changes on crop production and formulating corresponding agricultural measures, offering a time-efficient and cost-effective approach. Integrating process-based crop models with climate models has been widely adopted by scholars globally. Due to variations in the applied crop models, climate models, and regional conditions, simulations of cotton yield and water consumption exhibit notable differences. For instance, Li et al. [8] conducted field experiments in central-eastern Texas, utilizing the APSIM model to simulate the impact of climate change on cotton yield and water use efficiency, revealing significant declines in both metrics under future climate scenarios. Luo et al. [9] simulated climate change and cotton water consumption across nine cotton-growing regions in eastern Australia using the CSIRO OZCOT model, indicating increased temperatures and precipitation, with irrigated cotton yields improving by 0-25% and water consumption rising by 0-4%. Chen et al. [10] combined the RZWQM2 model with six global climate models to predict the effects of climate change on cotton yield and water requirements in the Cele Oasis, Xinjiang, showing that lint cotton yields would increase by 5.6% and 4.5% under RCP4.5 and RCP8.5 scenarios respectively during 2041-2060, while water requirements would decrease by 7.5% and 10.3%. Rahman et al. [11] used the CROPGRO-Cotton model to predict future climate impacts on cotton production in Pakistan, demonstrating mean seed cotton yield decrease by 12% and 30% under the RCP 8.5 scenario. In these studies focusing on cotton production forecasts within research areas, employing multiple climate models and scenarios is a common strategy to reduce errors and uncertainties. However, over 80% of studies focus on single regions, neglecting comparative analyses across agroecological zones [12].

1.3. Impacts of Climate Change on Cotton Growth and Water Consumption

Climate change exerts multifaceted impacts on cotton production through dynamic interactions between atmospheric, hydrological, and biological factors. The primary mechanisms manifest through two key drivers: temperature elevation and CO_2 concentration increase, with water availability serving as a critical mediating factor [13-15]. Rising temperatures accelerate cotton's phenological development, compressing its growth cycle [16, 17]. While this thermal acceleration might theoretically enhance growth rates, practical outcomes reveal significant trade-offs. Extreme heat events disrupt reproductive processes, inducing boll shedding and yield reduction through physiological stress [18, 19]. Concurrently, elevated temperatures amplify evapotranspiration demands [9], exacerbating water scarcity particularly in arid production regions.

Elevated atmospheric CO_2 concentrations counteract thermal stresses through distinct physiological mechanisms. By enhancing ribulose-1,5-bisphosphate carboxylase/oxygenase (Rubisco) activity, CO_2 enrichment improves photosynthetic carbon assimilation rates, while simultaneously reducing stomatal aperture and transpirational water loss [20, 21]. This dual effect promotes dry matter accumulation in cotton plants, particularly under water-limited conditions, as demonstrated by a 12–18% increase in biomass production in free-air CO_2 enrichment (FACE) experiments [22, 23]. However, the compensatory capacity of CO_2 fertilization is constrained by co-limiting factors: nutrient deficiencies (e.g., nitrogen) can reduce photosynthetic gains by 40 – 60%, while water scarcity thresholds determine whether CO_2-induced water savings translate to yield benefits [24, 25]. Experimental evidence suggests that CO_2 enrichment may offset 10–30% of yield

 doi:10.20944/preprints202503.2226.v1

losses caused by moderate warming, but this mitigation potential diminishes under extreme heat (>35°C) or prolonged drought, highlighting its context-dependent nature.

Process-based crop models reveal the emergent outcomes of interacting climate drivers, challenging single-factor predictions. The GOSSYM model simulations for Mississippi cotton systems demonstrated that CO_2 enrichment alone increased yields by 10% through enhanced photosynthesis, yet concurrent warming (+3°C) and precipitation variability (−15%) reversed this gain, resulting in a net 9% yield decline [26]. Similarly, LPJmL model projections for 2050 showed that excluding CO_2 effects led to a 14% yield reduction from climate change, whereas incorporating CO_2 fertilization reversed this trend, projecting a 6% net increase [12]. These results are in agreement with multi-model syntheses indicating that CO_2 benefits dominate under moderate warming (+2°C) but are negated by extreme heat waves exceeding crop thermal thresholds [27, 28]. Such findings underscore the necessity of integrating dynamic CO_2, temperature and precipitation interactions, region-specific cultivar adaptations, and stochastic extreme event modules in predictive frameworks to avoid systematic underestimation of climate risks.

1.4. Objective of the Study

This study seeks to improve climate impact assessments on cotton production in China by addressing existing gaps through three key approaches. First, we utilize 22 Coupled Model Intercomparison Project Phase 6 (CMIP6) General Circulation Models (GCMs) across four Shared Socioeconomic Pathways (SSPs) — SSP1-2.6, SSP2-4.5, SSP3-7.0, and SSP5-8.5 — to generate probabilistic projections that comprehensively capture the uncertainty space of future climate scenarios. This approach provides a robust foundation for understanding the range of potential climate impacts on cotton yields. Second, we focus on China's three major cotton-producing regions—the Xinjiang oasis, the Yellow River basin, and the Yangtze River basin—to identify region-specific vulnerabilities and adaptation needs. By analyzing these distinct agroecological zones, we aim to provide targeted insights for climate-resilient cotton production. Third, we quantify the relative contributions of key climatic factors—temperature, radiation, CO_2 concentration, and precipitation — to yield variability, offering a detailed understanding of the drivers of cotton productivity under changing climate conditions. Together, these advancements aim to inform sustainable agricultural practices and policy decisions in the face of climate uncertainty.

2. Materials and Methods

2.1. Study Area

The experiment was conducted at the Wangdu Irrigation Station (38.72°N, 115.12°E, 45.9 m asl), a field site of the Baoding Water Conservancy Bureau, over two consecutive cropping years (2018–2019 and 2019–2020). The site lies in a medium-temperate to sub-humid climatic zone, with a long-term annual mean air temperature of 11.8°C and annual mean precipitation of 507.5 mm, 80% of which occurs from June to September. Precipitation during the winter wheat season was 87.8 mm in 2018–2019 and 126.5 mm in 2019–2020 (Figure 1). The soil type is cinnamon soil, with a bulk density of 1.48 g/cm^3 and a field capacity water content of 0.27 m^3/m^3 in the 0–20 cm soil layer. The clay (<0.002 mm), silt (0.002–0.05 mm), and sand (0.05–2 mm) fractions were 0.021, 0.306, and 0.673, respectively. The soil contained 1.24% organic matter, with available nitrogen (N), phosphorus (P), and potassium (K) contents of 105.64, 17.46, and 95.05 mg/kg, respectively.

The Northwest Inland, Yangtze River Basin, and Yellow River Basin are the three major cotton planting regions in China. We selected three representative sites: Aral Station (Irrigation Experiment Station of the First Agricultural Division) for the Northwest Inland, Wangdu Station (Baoding Irrigation Experiment Station) for the Yellow River Basin, and Changde Station (National Meteorological Station) for the Yangtze River Basin. The geographical locations of these study areas are shown in Figure 1.

 doi:10.20944/preprints202503.2226.v1

Aral Station (40°33′N, 81°16′E, 1012.2 m asl) is located in southern Xinjiang Uygur Autonomous Region, characterized by a warm temperate extreme continental arid desert climate with an average annual temperature of 11.4°C and annual precipitation of 49 mm. The region experiences high evaporation and low precipitation, relying on irrigation from surrounding mountain glacier/snowmelt water. The soil is predominantly alluvial, with light sandy textures and significant salinization. Due to abundant sunlight and irrigation resources, the Xinjiang Cotton Region has become China's primary long-staple cotton production base, accounting for over 90% of national cotton production in 2022.

Wangdu Station (38°41′N, 115°08′E, 40.09 m asl) is situated in Wangdu County, Hebei Province, within a piedmont plain depression at the terminus of an alluvial fan. It features a typical warm temperate semi-humid monsoon climate with an average annual temperature of 11.8°C, wind speed of 2 m/s, precipitation of 507.5 mm, and 2580 annual sunshine hours. The growing season coincides with the periods of rain and heat. The brown loamy soil contains 1.24% organic matter, with available nitrogen (48.64 mg·kg^{-1}), phosphorus (17.46 mg·kg^{-1}), and potassium (95.05 mg·kg^{-1}). According to the China Statistical Yearbook (2023), Hebei Province had a cotton planting area of 116,100 hm^2 in 2022, representing 3.87% of the national total and ranking second only to Xinjiang.

Changde Station (29°03′N, 111°41′E, 35 m asl) lies in northwestern Hunan Province, a transitional central-to-north subtropical monsoon humid climate zone with plains, mountains, and hills. The region has an average annual temperature of 16.7°C and annual rainfall of 1200–1900 mm. Cotton cultivation is concentrated in four northern counties (Anxiang, Lixian, Nan, and Huarong), covering approximately 64,600 hm^2 in 2022.

These three sites were selected for their high cotton yields and significant planting area proportions within their respective regions, making them representative of China's three major cotton production zones.

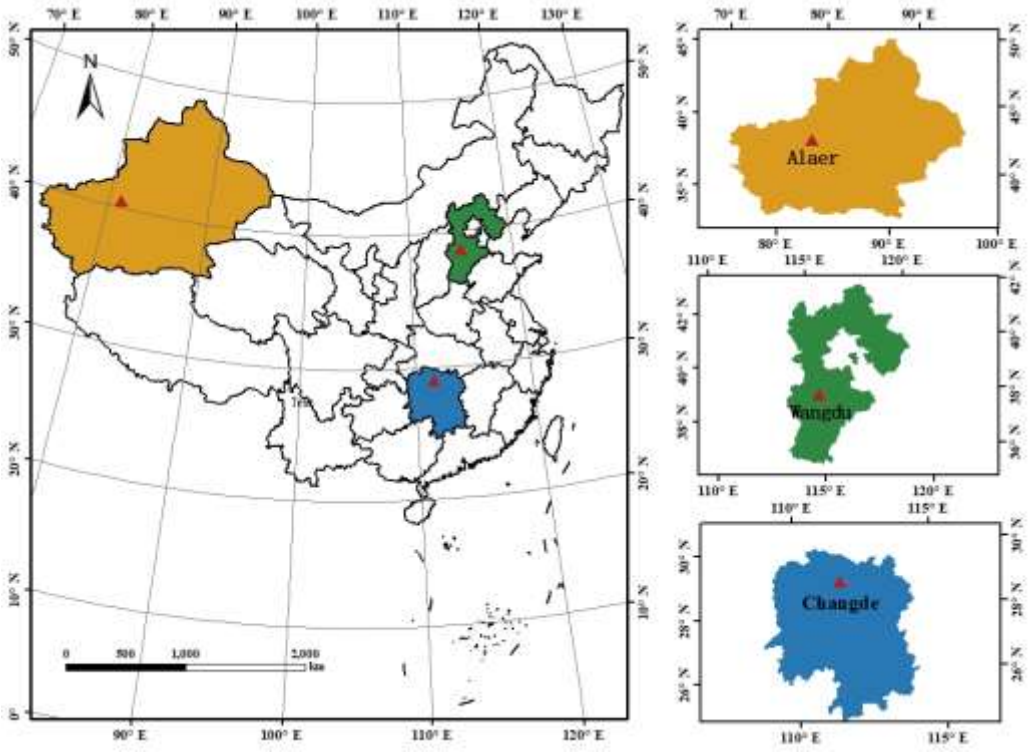

Figure 1. Geographical locations of the three sites.

2.2. Brief Introduction of APSIM-COTTON

APSIM (Agricultural Production Systems Simulator) is an agricultural production systems simulator developed by CSIRO (Commonwealth Scientific and Industrial Research Organisation)

 doi:10.20944/preprints202503.2226.v1

and APSRU (the Queensland Government's Agricultural Production Systems Research Group). The effects of climate, genotype, soil, and agricultural management practices on crop production can be modeled [29]. Since its establishment in 1996, the model has evolved from a planting system model to an agro-ecosystem model. APSIM provides a basic framework that includes biophysical modules, management modules, data input and output modules, and simulation engines that drive the simulation process and control all information exchange between individual modules, allowing data to be exchanged between them. APSIM takes the soil module as the core and simulates crop growth and development through coupling with the crop module, which is its unique advantage over other crop models. APSIM has a strong ability to simulate the adjustment of crop planting structures, crop growth and development, yield prediction, and water resource management for different planting methods under various soil conditions in different climatic zones. As one of the models in the APSIM series, the APSIM-COTTON model is not only sensitive to yield changes and economic risks under extreme environmental conditions but can also simulate soil production potential under the influence of decision management practices such as cotton rotation and intercropping. The APSIM-COTTON model is highly targeted, featuring a relatively simple mechanistic approach that enables precise assessment of the effects of climatic variations, soil conditions, and management practices on the present and projected productivity of cotton cultivation systems.

The APSIM-COTTON model mainly involves three modules: crop, soil, and management [30]. Among them, the crop module is mainly used to simulate cotton development and yield formation, including parameters related to crop varieties such as lint percentage, respiratory constant, leaf area growth rate, etc. The soil module primarily includes processes such as soil water balance and the transport and transformation of nitrogen, phosphorus, etc. The soil water module involves a series of processes such as precipitation, evapotranspiration, irrigation, runoff, and drainage. The management module facilitates user customization of variables, access to system-defined parameters, and redefinition of the simulation process in accordance with specific agricultural production scenarios. Key components of this module encompass sowing, irrigation, fertilization, harvesting, and other essential management practices.

2.3. Data resources

2.3.1. Meteorological Data

Historical climate data, including daily precipitation (mm), sunshine duration (hours), maximum temperature (°C), minimum temperature (°C), and other meteorological indices from 1961 to 2012, were obtained from the China Meteorological Science Data Sharing Service Network (CMDSSS) (http://cdc.cma.gov.cn/home.do). Sunshine duration data were subsequently converted into solar radiation ($MJ \cdot m^{-2}$) using the method proposed by Brock [31].

For future climate projections, data from the Coupled Model Intercomparison Project Phase 6 (CMIP6) dataset, encompassing 22 Global Climate Models (GCMs), were utilized (available at http://esgf-node.llnl.gov/search/cmip6/). Table 1 provides detailed information on these GCMs. This study selected four representative climate scenarios from the GCMs based on the Intergovernmental Panel on Climate Change (IPCC) Special Report on Emissions Scenarios: SSP5-8.5 (high emissions scenario), SSP3-7.0 (high emissions scenario), SSP2-4.5 (medium emissions scenario), and SSP1-2.6 (low emissions scenario).

Statistical downscaling data were provided by Deli Liu, a researcher at the Wagga Wagga Agricultural Research Institute, Department of Primary Industries (DPI), Australia. This dataset employs the NWAI-WG statistical downscaling method [32]. Through this method, data from three stations were spatially and temporally downscaled to generate daily station climate data. Initially, the monthly General Circulation Model (GCM) data were downscaled to site-specific monthly data by integrating spatial interpolation with bias correction techniques, calibrated against observational data spanning from 1961 to 2010. Subsequently, the refined site-specific monthly data were disaggregated into daily data using an enhanced version of the WGEN weather generator [33].

 doi:10.20944/preprints202503.2226.v1

Table 1. Information of the 22 Global Climate Models (GCMs) applied in the study.

Number	Code	Name	Institution	Country
1	ACC1	ACCESS-CM2	CSIRO-ARCCSS-BoM	Australia
2	ACC2	ACCESS-ESM1-5	CSIRO	Australia
3	BCC	BCC-CSM2-MR	BCC	China
4	Can1	CanESM5	CCCMA	Canada
5	Can2	CanESM5-CanOE	CCCMA	Canada
6	CNR1	CNRM-ESM2-1	CNRM-CERFACS	France
7	CNR2	CNRM-CM6-1	CNRM-CERFACS	France
8	CNR3	CNRM-CM6-1-HR	CNRM-CERFACS	France
9	ECE1	EC-Earth3-Veg	EC-Earth-Consortium	EU
10	ECE2	EC-Earth3	EC-Earth-Consortium	EU
11	FGOA	FGOALS-g3	CAS	China
12	GFD	GFDL-ESM4	NOAA-GFDL	US
13	GISS	GISS-E2-1-G	NASA-GISS	US
14	INM1	INM-CM4-8	INM	Russia
15	INM2	INM-CM5-0	INM	Russia
16	LPSL	IPSL-CM6A-LR	LPSL	France
17	MIR1	MIROC6	MIROC	Japan
18	MIR2	MIROC-ES2L	MIROC	Japan
19	MPI1	MPI-ESM1-2-HR	MPI-M	Germany
20	MPI2	MPI-ESM1-2-LR	MPI-M	Germany
21	MTIE	MRI-ESM2-0	MIR	Japan
22	UKES	UKESM1-0-LL	MOHC	UK

2.3.2. Soil Data

The physical properties of a continuous soil layer are characterized by a set of parameters, including bulk density (g cm^{-3}), air-dry water content (mm mm^{-1}), wilting point (mm mm^{-1}), field capacity (mm mm^{-1}), saturated water content (mm mm^{-1}), pH value, and soil particle composition. With the exception of the wilting point—estimated by the crop model—all other soil parameters were determined experimentally through a sampling approach. Soil profiles were analyzed across a 2-meter depth, with increments of 15 cm for the 0-30 cm layer and 30 cm for the 30-200 cm layer in Aral and Wangdu.

For Changde, bulk density and particle size distribution data were obtained from a representative section of China's national soil database (https://soil.geodata.cn/). Other pertinent soil parameters were estimated using the SPAW model [34], based on bulk density and particle size distribution. Detailed parameter values are provided in Table 2.

Table 2. Soil parameters in the profiles.

	Depth	Bulk density	Air-dry water content	Wilting point	Field capacity	Saturated water content
Aral	cm	g·cm^{-3}	mm·mm^{-1}	mm·mm^{-1}	mm·mm^{-1}	mm·mm^{-1}
	0-15	1.200	0.060	0.080	0.280	0.350

 doi:10.20944/preprints202503.2226.v1

	15-30	1.200	0.060	0.120	0.300	0.380
	30-60	1.400	0.060	0.150	0.320	0.410
	60-90	1.490	0.060	0.080	0.280	0.350
	90-120	1.560	0.060	0.080	0.280	0.350
	120-150	1.470	0.060	0.080	0.280	0.350
	150-180	1.470	0.060	0.080	0.280	0.350
Wangdu	0-15	1.470	0.060	0.119	0.274	0.425
	15-30	1.460	0.059	0.119	0.273	0.448
	30-60	1.390	0.050	0.109	0.264	0.444
	60-90	1.510	0.060	0.109	0.274	0.430
	90-120	1.510	0.058	0.097	0.272	0.430
	120-150	1.553	0.055	0.097	0.269	0.414
	150-180	1.510	0.065	0.097	0.313	0.430
Changde	0-12	1.470	0.050	0.090	0.365	0.445
	12-25	1.480	0.059	0.090	0.365	0.442
	25-65	1.490	0.060	0.115	0.300	0.410
	65-100	1.510	0.062	0.115	0.290	0.400

2.3.3. Crop Data

To enhance the applicability of the APSIM-COTTON model for localization studies in Aral, Wangdu, and Changde, model parameters were calibrated using our field experimental data of Aral in 2011 and Wangdu in 2019. For detailed experimental setups and parameter calibration procedures, please refer to Yang et al. [30] and Wang et al. [35]. For Changde, calibration was conducted based on aggregated statistical data and literature-derived information. The selection of cultivar-specific parameters and agricultural management practices primarily relies on field trial results and local cotton farmers' established practices, while acknowledging potential limitations in broader representativeness. The calibrated model parameters for the three locations are summarized in Table 3.

Table 3. Cotton variety parameters in three sites for APSIM-COTTON.

Parameter	Unit	Description	Wangdu	Aral	Changde
Percent_l	%	Percent of lint	43	41	36
Scboll	g/Boll	Seed cotton per boll	3.8	5.5	5
Respcon		Respiration constant	0.01593	0.02500	0.02306
Sqcon		Rate of squaring in thermal time	0.0181	0.021	0.0116

 doi:10.20944/preprints202503.2226.v1

Fcutout		Constant relating timing of cutout to boll load	0.5411	0.4789	0.4789
Flai		Ratio of leaf area per site	0.52	0.87	0.87
DDISQ	℃·d	Thermal time between emergence and the first square	402	380	450
TIPOUT		Tipping out time	52	75	52
FRUDD(8)	℃·d	Thermal time for each cotton fruiting stage	50, 169, 329, 356, 499, 642, 857, 1099	50, 180, 380, 400, 570, 630, 900, 1115	50, 250, 330, 420, 512, 610, 820, 1050
BLTME(8)		Fraction of boll development in one day	0, 0, 0, 0.07, 0.21, 0.33, 0.55, 1	0, 0, 0, 0.07, 0.21, 0.33, 0.55, 1	0, 0, 0, 0.07, 0.21, 0.33, 0.55, 1
Dlds_max		Maximum LAI growth rate	0.12	0.10	0.23
Rate_emergence		Rate of emergence	1	1	1.2
Popcon		Plant population constant	0.03633	0.3633	0.03633
Fburr		Ratio of seed cotton to seed cotton and burr per boll	1.23	1.23	1.73
ACOTYL	mm^2	Area of cotyledons	525	525	525
RLAI		Growth rate of leaf area with water stress before squaring	0.01	0.01	0.01

2.4. Statistical Method

2.4.1. Multiple Linear Regression

Multiple linear regression (MLR) was employed to analyze the relationship between cotton yield and normalized meteorological factors—including solar radiation, minimum temperature, maximum temperature, precipitation, and CO_2 concentration—over the period 1961–2100. The MLR equation used in this study is formulated as follows:

 doi:10.20944/preprints202503.2226.v1

$$Y_c = aR + bT_{min} + cT_{max} + dP + eC \quad (1)$$

Where *Yc* represents cotton yield (kg ha^{-1}), and *R*, *T*min, *T*max, *P*, and *C* denote the normalized values of solar radiation (MJ m^{-2}), minimum temperature (°C), maximum temperature (°C), rainfall (mm), and CO_2 concentration (mmol L^{-1}) during the growth period, respectively. The coefficients *a*, *b*, *c*, *d*, and *e* represent the regression coefficients for each corresponding variable.

2.4.2. Contribution Percentage

The contribution percentage of each meteorological factor—solar radiation, minimum temperature, maximum temperature, precipitation, and CO_2 concentration—to cotton yield was quantified based on the regression coefficients obtained from the multiple regression equation. The contribution rate was calculated using the following formula:

$$n_1 = \frac{|a|}{|a|+|b|+|c|+|d|+|e|}$$

$$n_2 = \frac{|b|}{|a|+|b|+|c|+|d|+|e|}$$

$$\cdots$$

$$n_5 = \frac{|e|}{|a|+|b|+|c|+|d|+|e|} \quad (2)$$

where，$n_1, n_2, \ldots n_5$ refer to the contribution percentage of R、T_{min}、T_{max}、P、C to Y_c.

3. Results

3.1. Chang of Climate for the Three Sites

For daily maximum air temperature (Tmax), under the lower radiative forcing scenarios (SSP1-2.6 and SSP2-4.5), Changde exhibited the largest increase (5.97% to 14.55%), followed by Aral (6.16% to 14.13%), while Wangdu showed the smallest increase (5.43% to 13.21%). Under the higher radiative forcing scenarios (SSP3-7.0 and SSP5-8.5), the percentage increase for Aral was the highest (6.12% to 26.25%), followed by Changde (5.04% to 25.41%), with Wangdu recording the lowest increase (4.23% to 22.45%).

For daily minimum air temperature (Tmin), the percentage increase at all three stations was greater than that for Tmax. Among them, Aral experienced the most significant increase (30.21% to 129.48%), followed by Wangdu (18.28% to 70.43%), while Changde had the smallest increase (8.22% to 33.87%).

Table 4. The variation and rate of change of maximum and minimum temperature at the three sites.

	Scenario	Time	Aral	Wangdu	Changde
Maximum temperature（°C）		Baseline	19.17	18.8	21.27
	SSP1-2.6	2030	1.25(6.51%)	1.14(6.05%)	1.41(6.65%)
		2050	1.61(8.4%)	1.57(8.34%)	1.97(9.25%)
		2070	1.69(8.79%)	1.69(8.97%)	2.09(9.83%)
		2090	1.66(8.68%)	1.69(9.01%)	2.1(9.88%)
	SSP2-4.5	2030	1.18(6.16%)	1.02(5.43%)	1.27(5.97%)
		2050	1.79(9.34%)	1.55(8.22%)	2.01(9.47%)

 doi:10.20944/preprints202503.2226.v1

		2070	2.32(12.12%)	2.05(10.93%)	2.67(12.57%)
		2090	2.71(14.13%)	2.48(13.21%)	3.09(14.55%)
	SSP3-7.0	2030	1.17(6.12%)	0.8(4.23%)	1.07(5.04%)
		2050	1.93(10.05%)	1.51(8.01%)	1.89(8.9%)
		2070	2.87(14.99%)	2.28(12.11%)	2.9(13.65%)
		2090	3.91(20.4%)	3.16(16.82%)	4(18.81%)
	SSP5-8.5	2030	1.31(6.81%)	1.16(6.15%)	1.44(6.77%)
		2050	2.34(12.19%)	2.01(10.68%)	2.55(11.99%)
		2070	3.55(18.5%)	3.09(16.42%)	3.88(18.23%)
		2090	5.03(26.25%)	4.22(22.45%)	5.4(25.41%)
Minimum temperature (°C)		Baseline	3.94	8.05	13.89
	SSP1-2.6	2030	1.19(30.21%)	1.49(18.53%)	1.21(8.68%)
		2050	1.58(40.01%)	1.98(24.58%)	1.6(11.5%)
		2070	1.67(42.28%)	2.14(26.51%)	1.74(12.5%)
		2090	1.61(40.7%)	2.06(25.6%)	1.71(12.27%)
	SSP2-4.5	2030	1.2(30.44%)	1.47(18.28%)	1.14(8.22%)
		2050	1.82(46.23%)	2.18(27.07%)	1.74(12.55%)
		2070	2.36(59.93%)	2.75(34.19%)	2.26(16.26%)
		2090	2.72(68.85%)	3.27(40.58%)	2.64(18.97%)
	SSP3-7.0	2030	1.2(30.55%)	1.28(15.86%)	1(7.22%)
		2050	2.03(51.46%)	2.23(27.69%)	1.71(12.3%)
		2070	2.98(75.65%)	3.28(40.74%)	2.59(18.61%)
		2090	4.04(102.41%)	4.44(55.17%)	3.56(25.59%)
	SSP5-8.5	2030	1.35(34.34%)	1.61(19.97%)	1.31(9.45%)
		2050	2.37(60.19%)	2.77(34.42%)	2.24(16.13%)
		2070	3.62(91.78%)	4.17(51.8%)	3.4(24.47%)
		2090	5.11(129.48%)	5.67(70.43%)	4.71(33.87%)

Regarding solar radiation, the Aral region exhibited a decreasing trend across most scenarios, with variations ranging from -0.23% to -4.56%. Conversely, both the Wangdu and Changde regions showed an increasing trend in solar radiation, except under the SSP3-7.0 scenario. Notably, the increase percentage in solar radiation was more pronounced in Changde (1.69% to 13.75%) compared to Wangdu (0.39% to 9.56%).

With respect to precipitation, forecasts indicate an overall increase at all stations. Among these, Changde was projected to experience the smallest increase in precipitation, with a range of 3.18% to 21.50%. For Wangdu, the precipitation across all scenarios for the 2030s and throughout the periods under the SSP1-2.6 scenario was expected to surpass that of Aral. However, in the other three scenarios, excluding the 2030s, the increase percentage in precipitation in Wangdu (22.14% to 50.79%) was generally lower than that in Aral (26.91% to 46.06%).

Table 5. The variation in solar radiation and precipitation at the three sites.

	Scenario	Time	**Aral**	**Wangdu**	**Changde**
Radiation ($MJ \cdot m^{-2}$)		Baseline	15.92	13.63	10.84
	SSP1-2.6	2030	-0.05(-0.34%)	0.35(2.59%)	0.64(5.89%)
		2050	0.04(0.23%)	0.99(7.23%)	1.27(11.72%)

 doi:10.20944/preprints202503.2226.v1

		2070	0.12(0.77%)	1.19(8.74%)	1.36(12.54%)
		2090	0.26(1.63%)	1.3(9.56%)	1.49(13.75%)
	SSP2-4.5	2030	-0.26(-1.62%)	-0.12(-0.91%)	0.18(1.69%)
		2050	-0.26(-1.61%)	0.28(2.05%)	0.66(6.08%)
		2070	-0.19(-1.21%)	0.61(4.47%)	1.14(10.54%)
		2091	-0.15(-0.95%)	0.88(6.45%)	1.34(12.35%)
	SSP3-7.0	2030	-0.45(-2.85%)	-0.94(-6.87%)	-0.53(-4.92%)
		2050	-0.63(-3.97%)	-1.03(-7.54%)	-0.52(-4.78%)
		2070	-0.68(-4.29%)	-0.89(-6.50%)	-0.22(-1.99%)
		2090	-0.73(-4.56%)	-0.7(-5.17%)	0.08(0.7%)
	SSP5-8.5	2030	-0.37(-2.33%)	0.05(0.39%)	0.32(2.98%)
		2050	-0.38(-2.38%)	0.2(1.50%)	0.69(6.41%)
		2070	-0.43(-2.7%)	0.34(2.49%)	1.05(9.73%)
		2090	-0.5(-3.13%)	0.37(2.74%)	1.49(13.71%)
Precipitation（mm）		Baseline	55.3	548.6	1324.2
	SSP1-2.6	2030	5.34(9.64%)	96.29(17.55%)	97.01(7.33%)
		2050	6.81(12.3%)	130.17(23.73%)	164.07(12.39%)
		2070	10.46(18.91%)	129.57(23.62%)	233.32(17.62%)
		2090	8.66(15.65%)	124.73(22.74%)	219.64(16.59%)
	SSP2-4.5	2030	7.94(14.36%)	85.3(15.55%)	71.29(5.38%)
		2050	12.55(22.68%)	142.81(26.03%)	108.3(8.18%)
		2070	14.89(26.91%)	139.68(25.46%)	117.52(8.87%)
		2090	20.64(37.3%)	147.3(26.85%)	212.17(16.02%)
	SSP3-7.0	2030	8.96(16.19%)	106.9(19.49%)	42.06(3.18%)
		2050	17.52(31.66%)	121.44(22.14%)	70(5.29%)
		2070	20.89(37.75%)	178.19(32.48%)	150.27(11.35%)
		2090	23.58(42.61%)	222.28(40.52%)	224.79(16.98%)
	SSP5-8.5	2030	7.94(14.35%)	100.77(18.37%)	95.07(7.18%)
		2050	16.96(30.66%)	152.72(27.84%)	175.84(13.28%)
		2070	25.1(45.36%)	207.95(37.91%)	237.72(17.95%)
		2090	25.48(46.06%)	278.65(50.79%)	284.67(21.5%)

3.2. Change of the Phenology and Uncertainty

 doi:10.20944/preprints202503.2226.v1

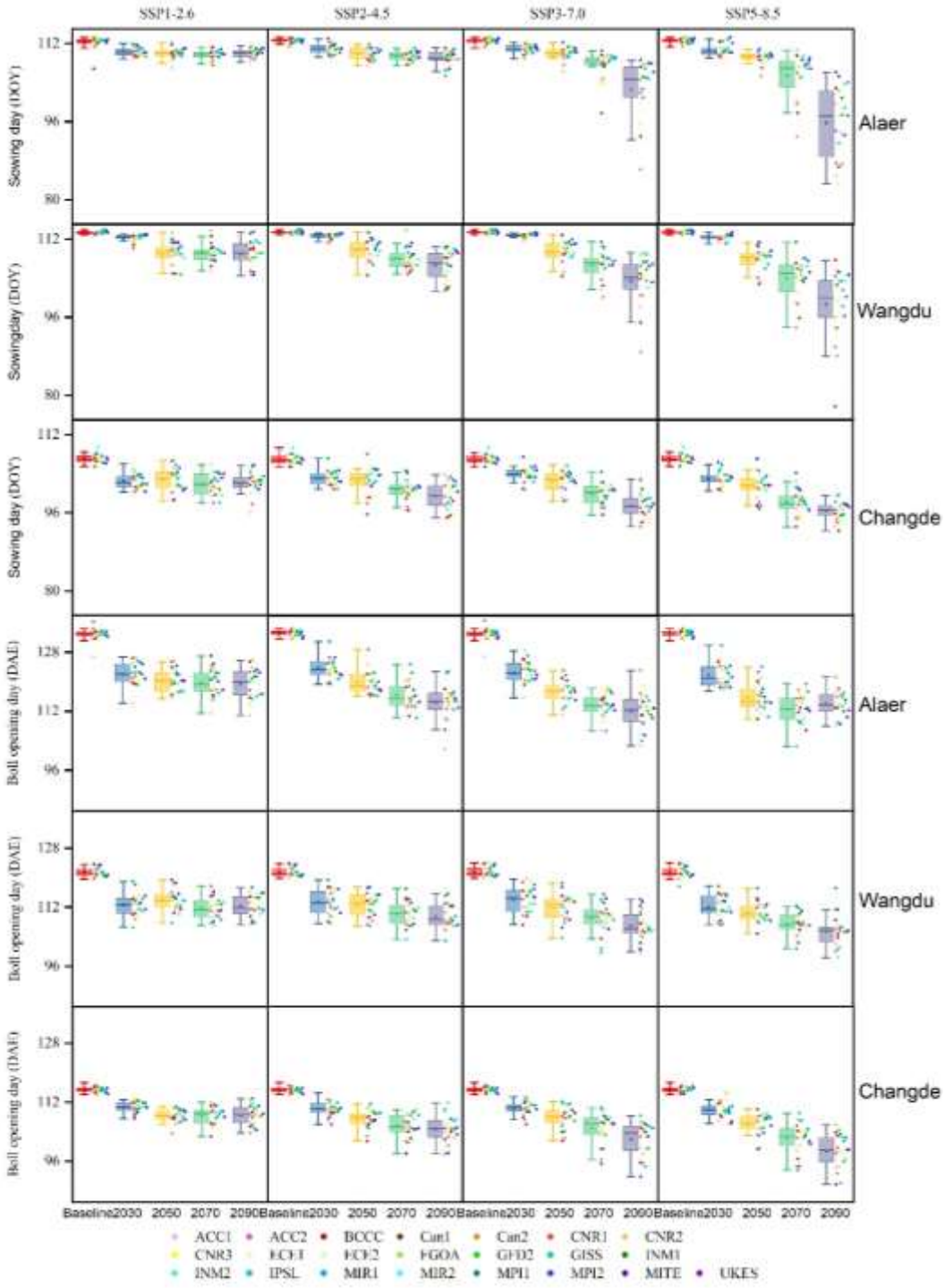

Figure 2. Predicted cotton phenology simulated by 22 GCMs under SSP1-2.6, SSP2-4.5, SSP3-7.0 and SSP5-8.5 climate scenarios in Aral, Wangdu and Changde.

The sowing dates at the three sites were observed to occur earlier compared to the baseline period, with advancements ranging from 1.7 to 16.8 days in Aral, 0.9 to 14.7 days in Wangdu, and 3.8 to 10.7 days in Changde (Figure 2). This trend towards earlier sowing was more pronounced with increasing radiative forcing and time progressing. Uncertainty by different GCMs also escalates with higher levels of radiative forcing and time passing. However, the response varies by location:

(1) For Aral, minimal inter-period differences were noted under the lower radiative forcing scenarios (SSP1-2.6 and SSP2-4.5). Conversely, under higher forcing scenarios (SSP3-7.0 and SSP5-8.5), the mean reduction in sowing days and variation (uncertainty) among different GCMs for the

 doi:10.20944/preprints202503.2226.v1

2070s and 2090s was considerably greater than 2030s and 2050s. (2) In Wangdu, the mean sowing date and variation in the 2030s showed little deviation from the baseline year. However, the changing magnitude of sowing date increased progressively with each subsequent 2-decade period in SSP2-4.5, SSP3-7.0 and SSP5-8.5. The uncertainty increases with time going in SSP5-8.5, and same trend was not found in other scenarios. However, in all scenarios, the uncertainty in 2090s was greater than the other periods. (3) In Changde, the sowing day was significantly earlier than that in baseline in all scenarios and periods. And the inter-periods variations in future was obvious in most scenarios except SSP1-2.6. The uncertainty in 2050s and 2070s (specially for 50% interquartile range) was greater than other periods most scenarios (except SSP2-4.5).

The analysis of uncertainty among the 3 sites indicates that the varied in Wangdu and Changde were greater than Aral in most periods and scenarios. However, in 2090s of SSP3-7.0 and SSP5-8.5, Aral was greater than Wangdu and Changde.

For the boll opening day, all three sites experienced an earlier onset compared to the baseline year, with the greatest advancement observed in Aral, followed by Wangdu, and the least in Changde. Under the SSP1-2.6 scenario, the mean differences in the boll opening stage across the four 2-decade were minimal. However, under the other three scenarios (SSP2-4.5, SSP3-7.0, and SSP5-8.5), the advancement in the boll opening date increased with both the passage of time and the increase in radiative forcing. The uncertainty in boll opening day generally increases from 2030 to 2090, especially under higher emission scenarios (SSP5-8.5). Aral shows higher uncertainty compared to Wangdu and Changde.

3.3. Change of the Yield and Uncertainty

In Aral, the yield under the SSP1-2.6 and SSP2-4.5 scenarios showed an increase of 3% to 10.6% compared to the baseline period (1690.7 kg·hm^{-2}). Under the higher radiative forcing scenarios SSP3-7.0 and SSP5-8.5, the yield initially increased before decreasing, leading to reductions of 11.6% and 24.5%, respectively, by the 2090s.

In the Wangdu and Changde, cotton yields exhibited minimal differences across decades under the low radiative forcing scenarios (SSP1-2.6 and SSP2-4.5). However, under high radiative forcing scenarios, there was a trend towards reduced yields. Specifically, under the SSP5-8.5 scenario, by the 2090s, yields decreased by 432.5 kg·hm^{-2} in Wangdu and 562.2 kg·hm^{-2} in Changde, relative to their respective baseline periods (1392.3 kg·hm^{-2} and 936.1 kg·hm^{-2}). The uncertainty in yield predictions generally increases from baseline to 2090, especially under higher emission scenarios (SSP5-8.5). Wangdu shows the greatest uncertainty, followed by Aral and Changde. Certain models (e.g., CNR1, CNR2) consistently show higher uncertainty across all sites and scenarios

 doi:10.20944/preprints202503.2226.v1

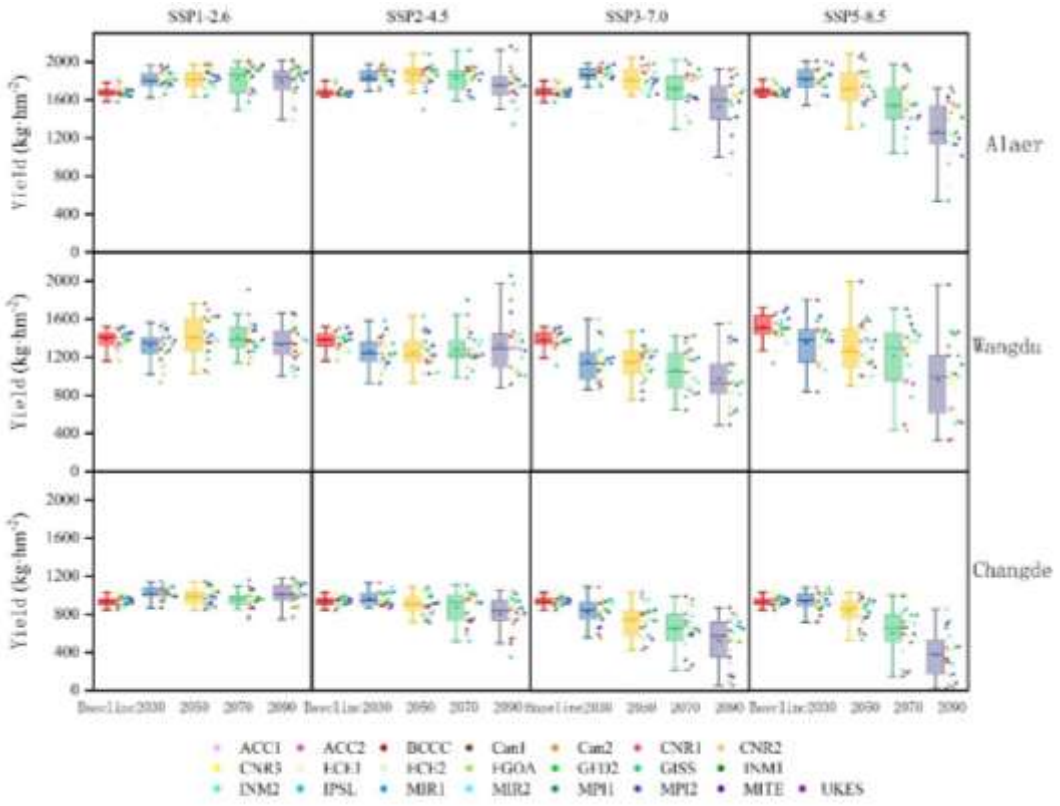

Figure 3. Predicted cotton yield simulated by 22 GCMs under SSP1-2.6, SSP2-4.5, SSP3-7.0 and SSP5-8.5 climate scenarios in Aral, Wangdu and Changde.

3.4. Change of the Water Use and Uncertainty

 doi:10.20944/preprints202503.2226.v1

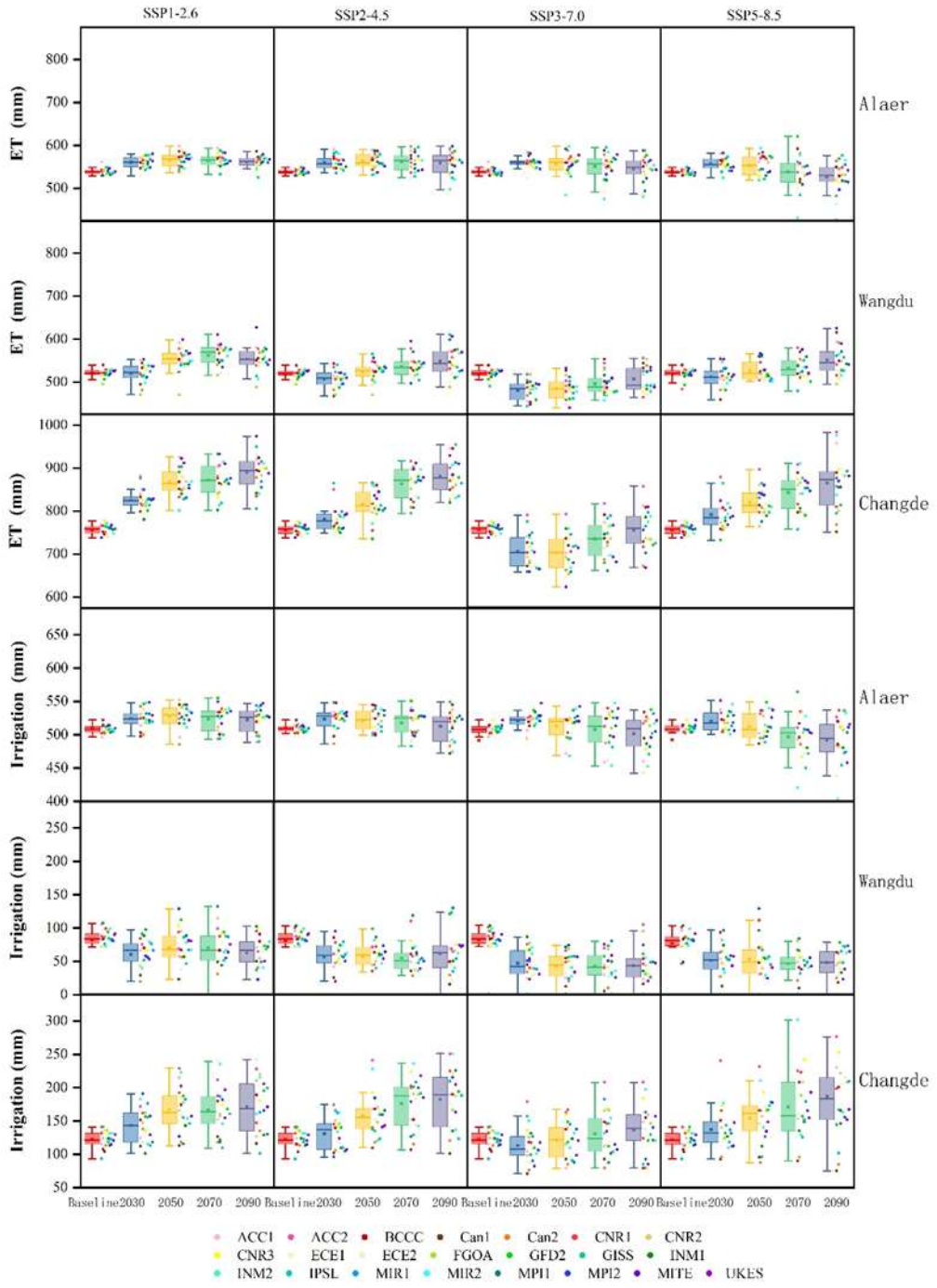

Figure 4. Prediction of cotton water use simulated by 22 GCMs under SSP1-2.6, SSP2-4.5, SSP3-7.0 and SSP5-8.5 climate scenarios in Aral, Wangdu and Changde.

In Aral, the ET in the future was slightly higher than the baseline in most scenarios, and there was little difference or a slight decrease over time. However, in Wangdu, the ET increased with time in most scenarios, and the ET projection was all greater than that in baseline, except SSP3-7.0. In Changde, the increasing trend was more obvious, except SSP3-7.0 in which the ET projection was less than baseline. Among the three sites, Changde exhibits the highest uncertainty in GCMs, followed by Wangdu, while Aral shows the least.

The irrigation amount in Aral in most future scenarios was greater than baseline, except SSP5-8.5 and decreased with time. In Wangdu, it was less than baseline and the difference among the future periods was small. However, there was a increasing trend in Changde and the difference among period was larger than that in Aral and Wangdu. And the uncertainty by the GCMs was greatest in Changde, followed by Wangdu and smallest in Aral.

 doi:10.20944/preprints202503.2226.v1

3.5. Contribution of climatic factors to cotton yield

Through correlation analysis of 4,400 simulation results from 100 years, 22 GCMs, and 4 scenarios at each site, the relationships between cotton yield and five major climate factors were determined (Table 3). Generally, across all sites, cotton yield showed a significant positive correlation with solar radiation and a negative correlation with maximum daily temperature. The relationship with minimum daily temperature was positive under most scenarios, and especially in the low radiative forcing scenarios. The relationship with precipitation varied by site: it was positively correlated in Aral and negatively correlated in Wangdu and Changde. Cotton yield was positively correlated with CO_2 concentration in most scenarios, except for Aral under the SSP3-7.0 and SSP5-8.5 scenarios, and Changde under the SSP5-8.5 scenario, where a negative correlation was observed.

Table 6. Coefficients of multiple linear regression analysis of cotton yield and climatic factors in Aral, Wangdu and Changde.

	Scenario	Radiation	Max T	Min T	Precipitation	[CO_2]
Aral	SSP1-2.6	0.12***	-0.2***	0.04	0.2***	0.19***
	SSP2-4.5	0.04**	-0.18***	0.18***	0.03	0.09***
	SSP3-7.0	0.07***	-0.42***	0.37***	0.005	-0.02
	SSP5-8.5	0.1***	-6.47	-4.73	10.73	-0.15***
	All	0.09***	-0.32***	0.45***	0.15***	-0.19***
Wangdu	SSP1-2.6	0.23***	-0.21***	0.22***	-0.94***	0.02
	SSP2-4.5	0.22**	-0.16**	0.12**	-0.87***	0.03
	SSP3-7.0	0.15***	0.02	-0.08	-0.8***	0.003
	SSP5-8.5	0.13***	-0.02	-0.11*	-1.04***	0.04
	All	0.21***	-0.1***	0.11***	-1.11***	-0.03
Changde	SSP1-2.6	0.37***	-0.24***	0.15***	-0.27***	0.003
	SSP2-4.5	0.41***	-0.54***	0.05	-0.31***	0.04*
	SSP3-7.0	0.42***	-0.73***	-0.11	-0.42***	0.08**
	SSP5-8.5	0.49***	-0.84***	0.01	-0.26***	-0.15***
	All	0.51***	-0.71***	0.19***	-0.27***	-0.22***

Note: Significance levels are denoted as follows: *** indicates $p<0.001$, ** indicates $p<0.01$, and * indicates $p<0.05$.

The contribution of different climatic factors to cotton yield varied across regions. In Aral, the daily maximum temperature, daily minimum temperature, and precipitation were the most significant contributors to yield. Under the SSP2-4.5 and SSP3-7.0 scenarios, the maximum and minimum temperatures had the greatest impact on cotton yield in Aral, with the maximum temperature exerting a negative influence of -34.97% and -47.28%, respectively, while the minimum temperature had a positive effect of 34.71% and 41.94%. Under the SSP1-2.6 and SSP5-8.5 scenarios, the precipitation during the growing season became the most influential factor, contributing 26.52% and 48.39%, respectively.

In Wangdu, precipitation was the dominant factor affecting yield across all four scenarios, with a consistently negative impact. The contribution of precipitation decreased from -58.02% under the low radiative forcing scenario (SSP1-2.6) to -77.23% under the high radiative forcing scenario (SSP5-8.5).

In Changde, the maximum temperature and solar radiation were the primary factors influencing cotton yield. The contribution of the maximum temperature was negative, ranging from -22.82% under the lowest radiative forcing scenario (SSP1-2.6) to -47.97% under the highest radiative forcing

 doi:10.20944/preprints202503.2226.v1

scenario (SSP5-8.5). Solar radiation had a positive impact, with contributions of 35.56%, 30.13%, 23.99%, and 27.95% across the four scenarios, respectively.

Table 7. Contribution of climatic fators to the cotton yield in Aral, Wangdu and Changde.

	Scenario	Radiation	Max T	Min T	Precipitation	[CO_2]
Aral	SSP1-2.6	16.57%	-26.14%	5.26%	26.52%	25.51%
	SSP2-4.5	7.88%	-34.97%	34.71%	5.86%	16.57%
	SSP3-7.0	8.37%	-47.28%	41.94%	0.54%	-1.87%
	SSP5-8.5	0.46%	-29.17%	-21.31%	48.39%	-0.67%
Wangdu	SSP1-2.6	14.35%	-12.94%	13.54%	-58.02%	1.15%
	SSP2-4.5	15.49%	-11.45%	8.79%	-61.96%	2.30%
	SSP3-7.0	14.43%	1.60%	-7.24%	-76.38%	0.35%
	SSP5-8.5	9.95%	-1.60%	-8.33%	-77.23%	2.88%
Changde	SSP1-2.6	35.56%	-22.82%	15.03%	-26.30%	0.29%
	SSP2-4.5	30.13%	-41.46%	3.91%	-22.97%	2.97%
	SSP3-7.0	23.99%	-41.46%	-6.13%	-24.07%	4.35%
	SSP5-8.5	27.95%	-47.97%	0.76%	-15.00%	-8.31%

4. Discussion

4.1. Strength and Limitation of the Study

This study utilized 22 Global Climate Models (GCMs) from the CMIP6 ensemble and multiple scenarios to assess the impact of future climate change on cotton growth and water consumption. Compared to previous studies, our approach significantly reduces uncertainties and errors in simulations. The following discussion will explore the main findings and their implications from various perspectives, incorporating additional literature to support our conclusions.

Previous research has often focused on a single cotton-growing region and used a limited number of GCMs for analysis, leading to significant uncertainties [2, 36]. By employing 22 GCMs and multiple scenarios, this study captures the complexity and diversity of climate change more comprehensively. Multi-model ensembles not only help reduce biases from individual models but also better reflect regional climate characteristics. For instance, across representative cotton-growing regions such as Aral, Wangdu, and Changde, we observed significant differences in how various climatic factors affect cotton yield and water consumption. This multi-model approach provides a more reliable scientific basis for future agricultural adaptation strategies [1, 4].

Despite the advantages of our multi-model ensemble approach, there are still limitations. Firstly, climate models inherently contain uncertainties, especially in predicting extreme weather events [1, 37]. Secondly, the environmental conditions, including climate, soil properties, and water availability, exhibit significant spatial heterogeneity even within the same cotton-growing region [38-40]. This spatial variability implies that data collected from a single site may not adequately represent the broader agricultural landscape, potentially limiting the generalizability of findings across different microclimates and soil types within the region. Finally, despite their widespread application in climate impact assessments, crop models exhibit several limitations when evaluating future climate scenarios [41]. One major constraint is the incomplete representation of complex plant physiological processes under extreme weather conditions, particularly regarding heat stress responses and CO_2 fertilization effects [42]. Current models often fail to adequately capture the non-linear interactions between temperature, water availability, and crop growth, potentially leading to inaccurate yield projections.

 doi:10.20944/preprints202503.2226.v1

4.2. Differences in Response to Climate Change in Different Regions

The heterogeneous impacts of climate change on cotton production across Aral, Wangdu, and Changde underscore the critical role of regional climatic baselines, agroecological contexts, and socioeconomic factors in shaping adaptive outcomes. While the study identifies distinct patterns in yield, phenology, evapotranspiration (ET), and irrigation demands, broader implications emerge when contextualizing these findings within global agricultural-climate literature, revealing both alignment and divergence with established theories.

The contrasting yield trends, with moderate increase in Aral under low radiative forcing versus severe declines in Wangdu and Changde under high radiation forcing scenarios, reflect a complex interplay among climatic factors. Similar patterns have been observed in other semi-arid regions, where moderate warming initially enhances photosynthesis but excessive heat disrupts reproductive stages [15]. However, the pronounced yield losses in Wangdu and Changde under SSP5-8.5 align with projections for regions with high baseline temperatures, where marginal increases in heatwaves disproportionately reduce crop productivity [43].

The advancement of sowing and boll opening dates is consistent with global observations of climate-driven phenological acceleration [44]. Studies in semi-arid regions, such as Asia, report similar phenological shifts due to warming temperatures [17, 45]. However, the magnitude of these shifts varies regionally, with higher uncertainty under extreme scenarios (SSP5-8.5), consistent with findings in other cotton-growing regions [9]. The minimal inter-period differences under low forcing scenarios in Aral contrast with studies in temperate regions, where even modest warming accelerates phenology [46].

The stability of ET in Aral despite rising temperatures challenges conventional models predicting increased ET under warming [47]. This anomaly may reflect reduced crop duration due to earlier maturity, a phenomenon documented in wheat systems [48]. Conversely, the rising ET in Changde corresponds to projections for humid regions, where higher vapor pressure deficits amplify water loss [49]. The divergent irrigation trends—declining in Wangdu but rising in Changde—highlight the dual role of ET and precipitation. The significant increase and greater variability in rainfall in Wangdu have led to heightened uncertainty in cotton production, suggesting that future climate change strategies in Wangdu should focus on enhanced water resource management.

4.3. Dominant Climate Drivers and Regional Specificity

The dominance of maximum temperature in Aral and solar radiation in Changde is consistent to global frameworks categorizing arid regions as temperature-limited and humid regions as radiation-limited [50]. However, the strong negative contribution of precipitation in Wangdu (-77% under SSP5-8.5) contrasts with studies in African semi-arid zones, where temperature often supersedes precipitation as a yield limiter [51]. Similar patterns are observed globally, where intense monsoon or summer rains disrupt cotton growth through multiple pathways. In the North China Plain, waterlogging caused by heavy rainfall suppresses root development and photosynthetic efficiency, leading to yield losses [52]. Excessive rainfall during flowering and boll formation stages increases boll shedding by up to 30% due to physical damage and nutrient leaching [53]. The positive correlation between minimum temperature and yield in Aral under low forcing scenarios parallels findings in Australian cotton systems, where nighttime warming extends frost-free periods [54], yet this benefit diminishes under extreme warming, highlighting threshold-based responses.

The regional disparities in climate responses demand context-specific adaptations. In Aral, breeding programs targeting heat-tolerant cultivars could mitigate yield losses, while Wangdu's water scarcity necessitates investments in drip irrigation and rainwater harvesting. Changde's radiation-driven systems may benefit from agroforestry to optimize light interception. Critically, these strategies must address compounding uncertainties by leveraging advances in climate-smart agriculture and decentralized governance frameworks. Future research should prioritize transdisciplinary collaborations to bridge the gap between model projections and on-ground realities, ensuring resilience in a warming world.

 doi:10.20944/preprints202503.2226.v1

5. Conclusions

Under scenarios characterized by increased temperatures and precipitation in all sites, and elevated solar radiation in Wangdu and Changde while decreased in Aral, cotton yields exhibited a declining trend under high radiative forcing conditions. Evapotranspiration (ET) increased across all locations, while irrigation amount decreased in Wangdu but increased in Changde and Aral. The variability in outcomes driven by different GCMs contributed significantly to the overall uncertainty of the results. Specifically, the uncertainties in yield and phenology were greatest in Wangdu, whereas Changde showed the highest uncertainties in ET and irrigation amount.

The relationship between cotton yield and various climatic factors was analyzed and the results indicate that, in most scenarios, cotton yields at all three sites exhibited a significant positive correlation with solar radiation during the growing season and a significant negative correlation with maximum temperature. Regarding the impact of CO_2 concentration, the analysis showed that at lower CO_2 levels, there was a positive correlation with cotton yield. However, at higher CO_2 concentrations, yield reductions were more likely to be influenced by temperature and precipitation rather than CO_2 itself. In Wangdu and Changde, cotton yields showed a significant negative correlation with precipitation, whereas in Aral, cotton yields displayed a positive correlation with precipitation.

6. Patents

Acknowledgments: This study was funded by Hebei Natural Science Foundation (Project No.: C2022503008) and the Natural Science Foundation of China (42207551).

Conflicts of Interest: The authors declare no conflicts of interest.

References

1. Semenov, M.A.; Stratonovitch, P. Use of multi-model ensembles from global climate models for assessment of climate change impacts. *Clim. Res.* **2010,** *41,* 1-14.
2. Abbasian, M.; Moghim, S.; Abrishamchi, A. Performance of the general circulation models in simulating temperature and precipitation over Iran. *Theor. Appl. Climatol.* **2018,** *135,* 1465-1483.
3. Soussana, J.F.; Graux, A.I.; Tubiello, F.N. Improving the use of modelling for projections of climate change impacts on crops and pastures. *J. Exp. Bot.* **2010,** *61,* 2217-2228.
4. Trnka, M.; Dubrovský, M.; Semerádová, D.; Žalud, Z. Projections of uncertainties in climate change scenarios into expected winter wheat yields. *Theor. Appl. Climatol.* **2004,** *77,* 229-249.
5. Wessolek, G.; Asseng, S. Trade-off between wheat yield and drainage under current and climate change conditions in northeast Germany. *Eur. J. Agron.* **2006,** *24,* 333-342.
6. Almazroui, M.; Saeed, F.; Islam, M.N.; Alkhalaf, A.K. Assessing the robustness and uncertainties of projected changes in temperature and precipitation in AR4 Global Climate Models over the Arabian Peninsula. *Atmos. Res.* **2016,** *182,* 163-175.
7. Nasim, W.; Amin, A.; Fahad, S.; Awais, M.; Khan, N.; Mubeen, M.; Wahid, A.; Rehman, M.H.; Ihsan, M.Z.; Ahmad, S.; et al. Future risk assessment by estimating historical heat wave trends with projected heat accumulation using SimCLIM climate model in Pakistan. *Atmos. Res.* **2018,** *205,* 118-133.
8. Li, Z.; Menefee, D.; Yang, X.; Cui, S.; Rajan, N. Simulating productivity of dryland cotton using APSIM, climate scenario analysis, and remote sensing. *Agr. Forest Meteorol.* **2022,** *325,* 109148.
9. Luo, Q.; Bange, M.; Johnston, D.; Braunack, M. Cotton crop water use and water use efficiency in a changing climate. *Agr. Ecosyst. Environ.* **2015,** *202,* 126-134.

 doi:10.20944/preprints202503.2226.v1

10. Chen, X.; Qi, Z.; Gui, D.; Gu, Z.; Ma, L.; Zeng, F.; Li, L. Simulating impacts of climate change on cotton yield and water requirement using RZWQM2. *Agr. Water Manage.* **2019,** *222,* 231-241.
11. Rahman, M.H.u.; Ahmad, A.; Wang, X.; Wajid, A.; Nasim, W.; Hussain, M.; Ahmad, B.; Ahmad, I.; Ali, Z.; Ishaque, W.; et al. Multi-model projections of future climate and climate change impacts uncertainty assessment for cotton production in Pakistan. *Agr. Forest Meteorol.* **2018,** *253-254,* 94-113.
12. Jans, Y.; von Bloh, W.; Schaphoff, S.; Müller, C. Global cotton production under climate change – Implications for yield and water consumption. *Hydrol. Earth. Syst. Sc.* **2021,** *25,* 2027-2044.
13. Berg, A.; Sultan, B.; de Noblet-Ducoudré, N. What are the dominant features of rainfall leading to realistic large-scale crop yield simulations in West Africa? *Geophys. Res. Lett.* **2010,** *37,* L05405.
14. Ines, A.V.M.; Hansen, J.W.; Robertson, A.W. Enhancing the utility of daily GCM rainfall for crop yield prediction. *Int. J. Climatol.* **2011,** *31,* 2168-2182.
15. Lobell, D.B.; Sibley, A.; Ivan Ortiz-Monasterio, J. Extreme heat effects on wheat senescence in India. *Nat. Clim. Chang.* **2012,** *2,* 186-189.
16. Gérardeaux, E.; Sultan, B.; Palaï, O.; Guiziou, C.; Oettli, P.; Naudin, K. Positive effect of climate change on cotton in 2050 by CO2 enrichment and conservation agriculture in Cameroon. *Agron. Sustain. Dev.* **2013,** *33,* 485-495.
17. Wang, Z.; Chen, J.; Xing, F.; Han, Y.; Chen, F.; Zhang, L.; Li, Y.; Li, C. Response of cotton phenology to climate change on the North China Plain from 1981 to 2012. *Sci. Rep.* **2017,** *7,* 6628.
18. Cetin, O.; Basbag, S. Effects of climatic factors on cotton production in semi-arid regions-—A review. *Res. Crop.* **2010,** *11,* 785-791.
19. Singh, R.P.; Prasad, P.V.V.; Sunita, K.; Giri, S.N.; Reddy, K.R. Influence of High Temperature and Breeding for Heat Tolerance in Cotton: A Review. *Adv. Agron.* **2007,** *93,* 313-385.
20. Broughton, K.J.; Smith, R.A.; Duursma, R.A.; Tan, D.K.Y.; Payton, P.; Bange, M.P.; Tissue, D.T. Warming alters the positive impact of elevated CO2 concentration on cotton growth and physiology during soil water deficit. *Funct. Plant Biol.* **2017,** *44,* 267-278.
21. Kimball, B.A.; LaMorte, R.L.; Seay, R.S.; Pinter, P.J.; Rokey, R.R.; Hunsaker, D.J.; Dugas, W.A.; Heuer, M.L.; Mauney, J.R.; Hendrey, G.R.; et al. Effects of free-air CO2 enrichment on energy balance and evapotranspiration of cotton. *Agr. Forest Meteorol.* **1994,** *70,* 259-278.
22. Bassu, S.; Brisson, N.; Durand, J.L.; Boote, K.; Lizaso, J.; Jones, J.W.; Rosenzweig, C.; Ruane, A.C.; Adam, M.; Baron, C.; et al. How do various maize crop models vary in their responses to climate change factors? *Glob. Chang. Biol.* **2014,** *20,* 2301-2320.
23. Chun, J.A.; Wang, Q.; Timlin, D.; Fleisher, D.; Reddy, V.R. Effect of elevated carbon dioxide and water stress on gas exchange and water use efficiency in corn. *Agr. Forest Meteorol.* **2011,** *151,* 378-384.
24. Amthor, J.S. Effects of atmospheric CO2 concentration on wheat yield: review of results from experiments using various approaches to control CO2 concentration. *Field Crop. Res.* **2001,** *73,* 1-34.
25. Long, S.P.; Ainsworth, E.A.; Leakey, A.D.B.; Nösberger, J.; Ort, D.R. Food for thought: Lower-than-expected crop yield stimulation with rising CO2 concentrations. *Science* **2006,** *312,* 1918-1921.
26. Reddy, K.R.; Doma, P.R.; Mearns, L.O.; Boone, M.Y.L.; Hodges, H.F.; Richardson, A.G.; Kakani, V.G. Simulating the impacts of climate change on cotton production in the Mississippi Delta. *Clim. Res.* **2002,** *22,* 271-281.

 doi:10.20944/preprints202503.2226.v1

27. Adhikari, P.; Ale, S.; Bordovsky, J.P.; Thorp, K.R.; Modala, N.R.; Rajan, N.; Barnes, E.M. Simulating future climate change impacts on seed cotton yield in the Texas High Plains using the CSM-CROPGRO-Cotton model. *Agr. Water Manage.* **2016,** *164,* 317-330.
28. Roudier, P.; Sultan, B.; Quirion, P.; Berg, A. The impact of future climate change on West African crop yields: What does the recent literature say? *Global Environ. Chang.* **2011,** *21,* 1073-1083.
29. Keating, B.A.; Carberry, P.S.; Hammer, G.L.; Probert, M.E.; Robertson, M.J.; Holzworth, D.; Huth, N.I.; Hargreaves, J.N.G.; Meinke, H.; Hochman, Z.; et al. An overview of APSIM, a model designed for farming systems simulation. *Eur. J. Agron.* **2003,** *18,* 267-288.
30. Yang, Y.; Yang, Y.; Han, S.; Macadam, I.; Liu, D.L. Prediction of cotton yield and water demand under climate change and future adaptation measures. *Agr. Water Manage.* **2014,** *144,* 42-53.
31. Brock, T.D. Calculating solar radiation for ecological studies. *Ecol. Model.* **1981,** *14,* 1-19.
32. Liu, D.L.; Zuo, H. Statistical downscaling of daily climate variables for climate change impact assessment over New South Wales, Australia. *Clim. Change* **2012,** *115,* 629-666.
33. Richardson, C.W.; Wright, D.A. WGEN: A Model for Generating Daily Weather Variables. U. S. Department of Agriculture. *Agricultural Research Service* **1984,** *ARS-8,* 83.
34. Saxton, K.E.; Rawls, W.J. Soil Water Characteristic Estimates by Texture and Organic Matter for Hydrologic Solutions. *Soil Sci. Soc. Am. J.* **2006,** *70,* 1569-1578.
35. Wang, K.; Yang, Y.M.; Yang, Y.H.; Liu, D.L.; Chen, L. Evaluation of the effect of future climatic change on Hebei cotton production and water consumption using multiple GCMs. *Chinese Journal of Eco-Agriculture* **2023,** *31,* 845−857.
36. Almazroui, M.; Nazrul Islam, M.; Saeed, S.; Alkhalaf, A.K.; Dambul, R. Assessment of Uncertainties in Projected Temperature and Precipitation over the Arabian Peninsula Using Three Categories of Cmip5 Multimodel Ensembles. *Earth Syst. Environ.* **2017,** *1,* 23.
37. Christensen, J.H.; Hewitson, B.; Busuioc, A.; Chen, A.; Gao, X.; Held, I.; Jones, R.; Kolli, R.K.; Kwon, W.-T.; Laprise, R.; et al. Regional Climate Projections.In *Climate Change 2007: The Physical Science Basis;* Solomon, S., Qin, D., Manning, M., Chen, Z., Marquis, M., Averyt, K.B., Tignor, M., Miller, H.L., Eds.; Cambridge University Press: Cambridge, United Kingdom and New York, USA, 2007, pp. 847-940.
38. Hebbar, K.B.; Venugopalan, M.V.; Prakash, A.H.; Aggarwal, P.K. Simulating the impacts of climate change on cotton production in India. *Clim. Change* **2013,** *118,* 701-713.
39. Lobell, D.B.; Ortiz-Monasterio, J.I.; Asner, G.P.; Matson, P.A.; Naylor, R.L.; Falcon, W.P. Analysis of wheat yield and climatic trends in Mexico. *Field Crop. Res.* **2005,** *94,* 250-256.
40. Yang, X.; Chen, F.; Lin, X.; Liu, Z.; Zhang, H.; Zhao, J.; Li, K.; Ye, Q.; Li, Y.; Lv, S.; et al. Potential benefits of climate change for crop productivity in China. *Agr. Forest Meteorol.* **2015,** *208,* 76-84.
41. Asseng, S.; Ewert, F.; Rosenzweig, C.; Jones, J.W.; Hatfield, J.L.; Ruane, A.C.; Boote, K.J.; Thorburn, P.J.; Rötter, R.P.; Cammarano, D.; et al. Uncertainty in simulating wheat yields under climate change. *Nat. Clim. Chang.* **2013,** *3,* 827-832.
42. Lobell, D.B.; Hammer, G.L.; McLean, G.; Messina, C.; Roberts, M.J.; Schlenker, W. The critical role of extreme heat for maize production in the United States. *Nat. Clim. Chang.* **2013,** *3,* 497-501.
43. Zhao, C.; Liu, B.; Piao, S.; Wang, X.; Lobell, D.B.; Huang, Y.; Huang, M.; Yao, Y.; Bassu, S.; Ciais, P.; et al. Temperature increase reduces global yields of major crops in four independent estimates. *Proc. Natl. Acad. Sci.* **2017,** *114,* 9326-9331.
44. Piao, S.; Liu, Q.; Chen, A.; Janssens, I.A.; Fu, Y.; Dai, J.; Liu, L.; Lian, X.; Shen, M.; Zhu, X. Plant phenology and global climate change: Current progresses and challenges. *Glob. Chang. Biol.* **2019,**

 doi:10.20944/preprints202503.2226.v1

25, 1922-1940.

45. Schierhorn, F.; Hofmann, M.; Adrian, I.; Bobojonov, I.; Müller, D. Spatially varying impacts of climate change on wheat and barley yields in Kazakhstan. *J. Arid Environ.* **2020,** *178,* 104164.
46. Richardson, A.D.; Keenan, T.F.; Migliavacca, M.; Ryu, Y.; Sonnentag, O.; Toomey, M. Climate change, phenology, and phenological control of vegetation feedbacks to the climate system. *Agr. Forest Meteorol.* **2013,** *169,* 156-173.
47. Jung, M.; Reichstein, M.; Ciais, P.; Seneviratne, S.I.; Sheffield, J.; Goulden, M.L.; Bonan, G.; Cescatti, A.; Chen, J.; de Jeu, R.; et al. Recent decline in the global land evapotranspiration trend due to limited moisture supply. *Nature* **2010,** *467,* 951-954.
48. Asseng, S.; Ewert, F.; Martre, P.; Rötter, R.P.; Lobell, D.B.; Cammarano, D.; Kimball, B.A.; Ottman, M.J.; Wall, G.W.; White, J.W.; et al. Rising temperatures reduce global wheat production. *Nat. Clim. Chang.* **2014,** *5,* 143-147.
49. Pan, N.; Feng, X.; Fu, B.; Wang, S.; Ji, F.; Pan, S. Increasing global vegetation browning hidden in overall vegetation greening: Insights from time-varying trends. *Remote Sens. Environ.* **2018,** *214,* 59-72.
50. Challinor, A.J.; Watson, J.; Lobell, D.B.; Howden, S.M.; Smith, D.R.; Chhetri, N. A meta-analysis of crop yield under climate change and adaptation. *Nat. Clim. Chang.* **2014,** *4,* 287-291.
51. Baethgen, W.E. Climate Risk Management for Adaptation to Climate Variability and Change. *Crop Sci.* **2010,** *50,* S-70-S-76.
52. Wang, X.; Deng, Z.; Zhang, W.; Meng, Z.; Chang, X.; Lv, M. Effect of Waterlogging Duration at Different Growth Stages on the Growth, Yield and Quality of Cotton. *PLoS One* **2017,** *12,* e0169029.
53. Tariq, M.; Yasmeen, A.; Ahmad, S.; Hussain, N.; Afzal, M.N.; Hasanuzzaman, M. Shedding of Fruiting Structures in Cotton: Factors, Compensation and Prevention. *Tropical and Subtropical Agroecosystems* **2017,** *20,* 251-262.
54. Welsh, J.M.; Taschetto, A.S.; Quinn, J.P. Climate and agricultural risk: Assessing the impacts of major climate drivers on Australian cotton production. *Eur. J. Agron.* **2022,** *140,* 126604.